Nonequilibrium sum rules for the retarded self-energy of strongly correlated electrons

V. Turkowski[*]

Department of Physics and Astronomy, University of Missouri, Columbia, Missouri 65211, USA

J. K. Freericks[†]

Department of Physics, Georgetown University, Washington, DC 20057, USA

We derive the first two moment sum rules of the conduction electron retarded self-energy for both the Falicov–Kimball model and the Hubbard model coupled to an external spatially uniform and time-dependent electric field (this derivation also extends the known nonequilibrium moment sum rules for the Green functions to the third moment). These sum rules are used to further test the accuracy of nonequilibrium solutions to the many-body problem; for example, we illustrate how well the self-energy sum rules are satisfied for the Falicov–Kimball model in infinite dimensions and placed in a uniform electric field turned on at time $t=0$. In general, the self-energy sum rules are satisfied to a significantly higher accuracy than the Green function sum rules.

PACS number(s): 71.27.+a, 71.10.Fd, 71.45.Gm, 72.20.Ht

I. INTRODUCTION

The theoretical description of nonequilibrium strongly correlated electron systems is one of the most important problems in condensed matter physics. This problem is not only an intellectual challenge but has the potential for many practical applications. Systems with strong electron correlations, such as heavy-fermion compounds, manganites, high-temperature superconductors, and strongly correlated oxide multilayers, demonstrate interesting and unusual properties, some of which have already been applied to electronic and magnetic devices. Due to the expectation for strong tunability of such systems, they are important candidates to be used in modern nanoelectronics, such as multilayered structures, quantum wires, and dots. Some of the properties of these materials can be exploited in spintronic and orbitronic devices, where the spin and orbital degrees of freedom are manipulated.[1] Since the size of modern electronic devices can be small ($\sim 10-100$ nm), the physical processes in these systems can become strongly nonequilibrium because they are exposed to strong external fields, which are generated by moderate external potentials (~ 1 V) placed over the nanoscale structures. The second consequence of a small system size is that the system will have enhanced quantum fluctuations. This makes it difficult to study different properties of the system, such as transport and optics, since we cannot use phenomenological approaches that rely on different relaxation times (Coulomb, phonon, etc.), which are longer than typical time scales in the system. Recently, much progress has been made in experimental short pulse laser techniques, which allow one to study ultrafast processes in different bulk systems and nanostructures. These experiments also need a theoretical interpretation.

Thus, it is important to have exact nonequilibrium solutions for correlated electron systems, which can serve as benchmarks for more general approximation methods. This problem is complicated even in the equilibrium case, due to the fact that one needs to treat the kinetic energy and the potential Coulomb energy terms in the Hamiltonian on equal footing. The simplest models for correlated electrons are the Hubbard model[2,3] and the Falicov–Kimball model[5] (which is a simplified version of the Hubbard model with localized spin-down electrons). The equilibrium solutions of these models are known only in the one-dimensional case, where an analytical Bethe ansatz approach[4] can be used for the Hubbard model and in the limit of infinite dimensions, where the dynamical mean-field theory (DMFT) can be applied[5,6] to both models.

Similar to the equilibrium case, much progress in studying nonequilibrium properties of correlated electron systems has been made in both cases of low and high dimensions. Different approaches, such as perturbation theory, equation of motion, and variational wave function methods, were applied to study the properties of strongly correlated systems in the case of quantum dot and chain systems (see, for example, Refs. 7–10). Recently, a nonequilibrium generalization of the Bethe anzatz technique was proposed[11] and simulations in one dimension with the density matrix renormalization group have been performed.[12] In the infinite-dimensional case, the nonequilibrium properties of the Hubbard[13,14] and Falicov–Kimball[15] models were studied by using second-order perturbation theory in U within DMFT. Recently, the Falicov–Kimball model was exactly solved[16–21] in the presence of a homogeneous time-dependent electric field and in the case of a sudden change in the interaction strength U.[22] In these papers, the nonequilibrium generalization of the DMFT approximation was proposed, which allows one to obtain the numerical solution of the nonequilibrium problem for the Falicov–Kimball model. The numerical method is based on the Kadnoff–Baym–Keldysh nonequilibrium Green function formalism when the nonequilibrium Green function is defined on the Kadanoff–Baym–Keldysh time contour. We studied different properties of the model when a constant electric field is switched on at a particular moment of time. We found that Bloch oscillations of the electric current can survive for a long time and develop beats with a period depending on the interaction strength; in addition, the Wannier–Stark peaks in the density of states can broaden and split

when the Coulomb interaction increases. It was also found that the Falicov–Kimball model does not switch from one equilibrium state to another when the interaction strength is suddenly changed.

Since most solutions of strongly correlated problems are numerical, it is important to develop tests that allow one to check the precision of those solutions. In equilibrium, one of the ways to check the accuracy is to calculate the spectral moments of the Green function[23] and compare them to exact results. Spectral moments have been used in many different contexts than just to test the numerical accuracy of numerical solutions. Harris and Lange[24] used spectral moments and a projection that forbids double occupancy to determine properties about the spectral moments of the individual Hubbard bands at strong coupling. They also determined the equilibrium Green function moments for the Falicov–Kimball model when they examined an alloy disorder Hamiltonian. Nolting[25] used the spectral moments to develop different strong-coupling-based approximations to the Green functions of the Hubbard model. This approach has been extended in many different directions to look for magnetic order or to improve iterated perturbation theory in the dynamical mean-field theory when away from particle-hole symmetry.[26–30] White[23] used the exact expressions for the zeroth and the first two spectral moments for the Hubbard model to estimate the accuracy of a quantum Monte Carlo solution of the two-dimensional Hubbard model. Usually, only the zeroth and the first two moments have been examined. However, as was argued in Refs. [28] and [29], it is also important to know the third spectral moment since it is connected with the spontaneous magnetic order in correlated systems, and knowledge of the zeroth and the first three moments also contain valuable information about the strongly correlated band structure. The authors of these papers have also established a relation between the zeroth and the first moment for the self-energy with the lowest moments for the Green functions. This allowed them to estimate the precision of the solution for the self-energy at high energies. Recently, interest in the self-energy spectral moments has been renewed, due to an application of these results to the description of experiments on the self-energy of high-temperature superconductors arising from angle-resolved photoemission.[31–33] While the retarded Green function moments we discuss here are appropriate for the full spectral function, the lesser moments (and the greater moments which can be extracted from the retarded and lesser moments) are appropriate for photoemission or inverse photoemission experiments. The recent work in Ref. [32] examines the lesser moments with a further strong-coupling projection that removes doubly occupied states. We do not examine these kinds of projections here. Instead, we focus on nonequilibrium effects.

The nonequilibrium case is more complicated than the equilibrium case. In nonequilibrium, all Green functions now depend on two time variables, as opposed to just the time difference in equilibrium. Nevertheless, exact expressions have been found[17] for the zeroth and the first two spectral moments of the nonequilibrium lesser and retarded Green functions for the Falicov–Kimball and the Hubbard models (coupled to a homogeneous and time-dependent electric field). The moments were also used to test the accuracy of the nonequilibrium solution to the Falicov–Kimball model in the limit of infinite dimensions.

In this paper, we generalize the results of Ref. [17] by deriving the third spectral moments for the retarded and the lesser Green functions and deriving expressions for the corresponding zeroth and the first spectral moments of the retarded self-energy for the Falicov–Kimball and Hubbard models. Similar to the zeroth and the first two retarded Green function moments, the third-order moment of the retarded Green function (Falicov–Kimball model) and the zeroth (both) and first (Falicov-Kimball model) moments of the retarded self-energy remain time independent. We apply these results to benchmark the precision of the DMFT solution of the Falicov–Kimball model in both the equilibrium case (at arbitrary doping) and the nonequilibrium case (at half-filling) when a constant electric field is switched on at a particular moment of time.

The rest of the paper is organized as follows. The equilibrium Falicov–Kimball and Hubbard models and their generalization to include the external electric field are presented in Sec. II. The results for the spectral moments are presented in Sec. III (Green functions) and Sec. IV (self-energies). In Sec. V, we give a brief description of the nonequilibrium DMFT formalism, present equilibrium and nonequilibrium solutions of the infinite-dimensional Falicov–Kimball model, and compare results for the moments obtained from the numerical solutions with the exact results. Our summary and conclusions are presented in Sec. VI.

II. HAMILTONIANS FOR THE MODELS IN EQUILIBRIUM AND IN A UNIFORM FIELD

The generalized equilibrium Hamiltonian for the spinless Falicov–Kimball and the spin one-half Hubbard models can be written in the following unified form:

$$\mathcal{H}(0) = -\sum_{ij} t_{ij} c_i^\dagger c_j - \sum_{ij} t_{ij}^f f_i^\dagger f_j - \mu \sum_i c_i^\dagger c_i - \mu_f \sum_i f_i^\dagger f_i$$
$$+ U \sum_i f_i^\dagger f_i c_i^\dagger c_i, \tag{1}$$

where in the case of the Hubbard model, the operators c_i (f_i) and $c_i^\dagger$ ($f_i^\dagger$) correspond to the spin-up (spin-down) electron annihilation and creation operators on site i. In this paper, we consider the case of a hypercubic lattice and assume that the electrons can hop to the nearest neighbor site. The corresponding hopping matrices are $t_{ij} = t_{ij}^f$ and the chemical potentials are $\mu = \mu_f$ for both kinds of electrons (Zeeman splitting can be incorporated by choosing different chemical potentials, but for simplicity, we keep them equal here). The last term in the Hamiltonian describes the local Coulomb repulsion between spin-up and spin-down electrons with a strength equal to U. The Hamiltonian in Eq. (1) also corresponds to the spinless Falicov–Kimball model when one sets $t_{ij}^f = 0$. In this case, the system consists of two kinds of electrons: itinerant c electrons and localized f electrons, which locally repel each other. In the case of the Falicov–Kimball model, we shall also put $\mu_f = 0$ for simplicity since the value of the chemical potential of the localized electrons is not

important for the spectral moments of c electrons, which we evaluate below.

The electric field $\mathbf{E}(\mathbf{r},t)$ can be introduced into the Hamiltonian by means of the Peierls substitution for the hopping matrices,[34]

$$t_{ij} \rightarrow t_{ij} \exp\left[-\frac{ie}{\hbar c} \int_{\mathbf{R}_i}^{\mathbf{R}_j} \mathbf{A}(\mathbf{r},t)d\mathbf{r} \right] = \tilde{t}_{ij}, \qquad (2)$$

$$t_{ij}^f \rightarrow t_{ij}^f \exp\left[-\frac{ie}{\hbar c} \int_{\mathbf{R}_i}^{\mathbf{R}_j} \mathbf{A}(\mathbf{r},t)d\mathbf{r} \right] = \tilde{t}_{ij}^f, \qquad (3)$$

where the electric vector potential $\mathbf{A}(\mathbf{r},t)$ is connected to the electric field in the following way:

$$\mathbf{E}(\mathbf{r},t) = -\frac{1}{c}\frac{\partial \mathbf{A}(\mathbf{r},t)}{\partial t}, \qquad (4)$$

and the scalar potential vanishes. This choice of the electromagnetic potential, when the scalar potential is set equal to zero, corresponds to the Hamiltonian gauge. For simplicity, we also assume that the electric field is spatially uniform and it lies along the direction of the elementary cell diagonal,

$$\mathbf{A}(\mathbf{r},t) = A(t)(1,1,\ldots,1). \qquad (5)$$

Neglecting the spatial dependence of the vector potential assumes that we ignore the magnetic field effects in the system [since the magnetic field is $\mathbf{H}(\mathbf{r},t)=\nabla\times\mathbf{A}(\mathbf{r},t)$] because the electric field is smooth enough in time that the transient magnetic field can be neglected. This can take place in nanostructures when an applied external potential produces an almost homogeneous electric field due to the small size of the system (see also the discussion in Ref. [17]).

The Hamiltonian (in the Schrödinger picture), which describes the electron system coupled to an external spatially independent electric field, has a rather simple form in the momentum representation (the creation and annihilation operators now create or annihilate electrons with definite momentum),

$$\mathcal{H}(\mathbf{A}) = \sum_{\mathbf{k}} \left\{ \epsilon\left[\mathbf{k} - \frac{e\mathbf{A}(t)}{\hbar c} \right] - \mu \right\} c_{\mathbf{k}}^{\dagger} c_{\mathbf{k}}$$
$$+ \sum_{\mathbf{k}} \left\{ \epsilon^f\left[\mathbf{k} - \frac{e\mathbf{A}(t)}{\hbar c} \right] - \mu_f \right\} f_{\mathbf{k}}^{\dagger} f_{\mathbf{k}}$$
$$+ U \sum_{\mathbf{p},\mathbf{k},\mathbf{q}} f_{\mathbf{p}+\mathbf{q}}^{\dagger} c_{\mathbf{k}-\mathbf{q}}^{\dagger} c_{\mathbf{k}} f_{\mathbf{p}}, \qquad (6)$$

where the free electron band structures are

$$\epsilon\left[\mathbf{k} - \frac{e\mathbf{A}(t)}{\hbar c} \right] = \epsilon^f\left[\mathbf{k} - \frac{e\mathbf{A}(t)}{\hbar c} \right]$$
$$= -2t\sum_{j=1}^{d} \cos\left\{ a\left[\mathbf{k}_j - \frac{e\mathbf{A}_j(t)}{\hbar c} \right] \right\}, \qquad (7)$$

d is the dimensionality of the system, and t is the corresponding hopping parameter. In the case of the Falicov–Kimball model, one has to put $\epsilon^f\{\mathbf{k}-[e\mathbf{A}(t)/\hbar c]\}-\mu_f=0$ in Eq. (6).

III. SPECTRAL MOMENTS FOR THE GREEN FUNCTIONS

In the case of nonequilibrium, there are two independent Green functions, which describe the properties of a many-body system. We use the retarded,

$$G_{\mathbf{k}}^R(t_1,t_2) = -i\theta(t_1-t_2)\langle[c_{\mathbf{k}}(t_1),c_{\mathbf{k}}^{\dagger}(t_2)]\rangle, \qquad (8)$$

and the lesser,

$$G_{\mathbf{k}}^{<}(t_1,t_2) = i\langle c_{\mathbf{k}}^{\dagger}(t_2)c_{\mathbf{k}}(t_1)\rangle, \qquad (9)$$

Green functions as the basis functions. The fermion operators on the right hand side of Eqs. (8) and (9) are in the Heisenberg representation and the averaging operation $\langle\cdots\rangle$ is performed with respect to the equilibrium Hamiltonian (corresponding to the initial conditions prior to the field being turned on). It is convenient to use the Green functions in Eqs. (8) and (9) since they have important physical interpretations. Namely, the poles of the retarded Green function define the energy levels of the system (and thereby determine the many-body density of states), and the equal-time lesser Green function describes the occupation of these levels (and hence determines the distribution function). In equilibrium, only one of these functions is independent since they are connected by a simple relation depending on the Fermi–Dirac distribution.

In order to calculate moments of the spectral functions at different values of time, it is convenient to introduce Wigner's time variables: the average time $T=(t_1+t_2)/2$ and the relative time $t=t_1-t_2$. The frequency dependence of a Green function can be calculated by Fourier transforming the Green function with respect to the relative-time coordinate, and the time evolution of the function is then described by the average time coordinate. In other words, the average time coordinate is associated with the physical time in the system. The spectral function for the retarded and the lesser Green functions can then be defined in the following way:

$$A_{\mathbf{k}}^{R,<}(T,\omega) = \frac{\eta}{\pi} \mathrm{Im} \int_{-\infty}^{\infty} dt e^{i\omega t} G_{\mathbf{k}}^{R,<}(T,t), \qquad (10)$$

where we have introduced a prefactor η, which is equal to -1 for the retarded Green function and 1 for the lesser Green function in order to have positive zeroth moments for both retarded and lesser Green functions (see below). The nth spectral moments that correspond to the spectral functions in Eq. (10) are defined to be

$$\mu_n^{R,<}(\mathbf{k},T) = \int_{-\infty}^{\infty} d\omega\, \omega^n A_{\mathbf{k}}^{R,<}(T,\omega). \qquad (11)$$

It is not difficult to show from Eqs. (10) and (11) that there exist the following relations that connect the moments with the corresponding Green functions:

$$\mu_n^{R,<}(\mathbf{k},T) = \frac{\eta}{\pi} \mathrm{Im} \int_{-\infty}^{\infty} d\omega \int_{-\infty}^{\infty} dt e^{i\omega t} i^n \frac{\partial^n}{\partial t^n} G_{\mathbf{k}}^{R,<}(T,t)$$

$$(12)$$

and

$$\mu_n^{R,<}(\mathbf{k},T) = 2\frac{\eta}{\pi}\,\mathrm{Im}\left[i^n\frac{\partial^n}{\partial t^n}G_{\mathbf{k}}^{R,<}(T,t)\right]_{t=0^+} \quad (13)$$

(for details, see Ref. 17). It is more convenient to use the expression in Eq. (12) for the retarded Green function and in Eq. (13) for the lesser Green function. The time derivatives with respect to the operators of the Green functions in Eqs. (8) and (9) can be expressed by taking commutators of the corresponding fermion operators with the Hamiltonian in the Heisenberg picture (the terms proportional to the time derivatives with respect to the theta function in the case of the retarded Green function do not contribute to the moments). This leads to the following expressions, which connect the zeroth and the first three spectral moments with specific correlation functions:

$$\mu_0^R(\mathbf{k},T) = \langle[c_k(T),c_k^\dagger(T)]\rangle, \quad (14)$$

$$\mu_1^R(\mathbf{k},T) = \frac{1}{2}[\langle[L^1c_k(T),c_k^\dagger(T)]\rangle - \langle[c_k(T),L^1c_k^\dagger(T)]\rangle], \quad (15)$$

$$\mu_2^R(\mathbf{k},T) = \frac{1}{4}[\langle[L^2c_k(T),c_k^\dagger(T)]\rangle - 2\langle[L^1c_k(T),L^1c_k^\dagger(T)]\rangle + \langle[c_k(T),L^2c_k^\dagger(T)]\rangle], \quad (16)$$

$$\mu_3^R(\mathbf{k},T) = \frac{1}{8}[\langle[L^3c_k(T),c_k^\dagger(T)]\rangle - 3\langle[L^2c_k(T),L^1c_k^\dagger(T)]\rangle + 3\langle[L^1c_k(T),L^2c_k^\dagger(T)]\rangle - \langle[c_k(T),L^3c_k^\dagger(T)]\rangle], \quad (17)$$

$$\mu_0^<(\mathbf{k},T) = 2\langle c_k^\dagger(T)c_k(T)\rangle, \quad (18)$$

$$\mu_1^<(\mathbf{k},T) = \langle c_k^\dagger(T)L^1c_k(T)\rangle - \langle[L^1c_k^\dagger(T)]c_k(T)\rangle, \quad (19)$$

$$\mu_2^<(\mathbf{k},T) = \frac{1}{2}[\langle c_k^\dagger(T)L^2c_k(T)\rangle - 2\langle[L^1c_k^\dagger(T)][L^1c_k(T)]\rangle + \langle[L^2c_k^\dagger(T)]c_k(T)\rangle], \quad (20)$$

$$\mu_3^<(\mathbf{k},T) = \frac{1}{4}[\langle c_k^\dagger(T)L^3c_k(T)\rangle - 3\langle[L^1c_k^\dagger(T)][L^2c_k(T)]\rangle + 3\langle[L^2c_k^\dagger(T)][L^1c_k(T)]\rangle - \langle[L^3c_k^\dagger(T)]c_k(T)\rangle], \quad (21)$$

where $L^nO=[\cdots[[O,\mathcal{H}_H(T)],\mathcal{H}_H(T)]\cdots\mathcal{H}_H(T)]$ is the multiple commutation operator with respect to the Hamiltonian (in the Heisenberg picture) performed n times; the operator $\mathcal{H}_H(T)$ is given by Eq. (6) with all fermionic operators replaced by the Heisenberg-picture operators evaluated at time T. The commutation relations can be directly evaluated because two fermionic operators at equal times (within the Heisenberg picture) satisfy the canonical commutation relations.

Evaluating the commutation and anticommutation operations in Eqs. (14)–(17) results in the following expressions for the retarded moments:

$$\mu_0^R(\mathbf{k},T) = 1, \quad (22)$$

$$\mu_1^R(\mathbf{k},T) = \{\varepsilon[\mathbf{k} - e\mathbf{A}(T)] - \mu\} + Un_f, \quad (23)$$

$$\mu_2^R(\mathbf{k},T) = \{\varepsilon[\mathbf{k} - e\mathbf{A}(T)] - \mu\}^2 + 2U\{\varepsilon[\mathbf{k} - e\mathbf{A}(T)] - \mu\}n_f + U^2n_f, \quad (24)$$

$$\mu_3^R(\mathbf{k},T) = \{\varepsilon[\mathbf{k} - e\mathbf{A}(T)] - \mu\}^3 + 3U\{\varepsilon[\mathbf{k} - e\mathbf{A}(T)] - \mu\}^2n_f + 3U^2\{\varepsilon[\mathbf{k} - e\mathbf{A}(T)] - \mu\}n_f + U^2\sum_{\mathbf{p},\mathbf{q}}\{\varepsilon^f[\mathbf{p} + \mathbf{q} - e\mathbf{A}(T)]$$
$$- 2\varepsilon^f[\mathbf{p} - e\mathbf{A}(T)] + \varepsilon^f[\mathbf{p} - \mathbf{q} - e\mathbf{A}(T)]\}\langle f_{\mathbf{p}}^\dagger f_{\mathbf{p}}\rangle(T) - U^2\sum_{\mathbf{p},\mathbf{q},\mathbf{q}'}\{\varepsilon^f[\mathbf{p} + \mathbf{q} - e\mathbf{A}(T)] - \varepsilon^f[\mathbf{p} + \mathbf{q} + \mathbf{q}' - e\mathbf{A}(T)]$$
$$- \varepsilon^f[\mathbf{p} - e\mathbf{A}(T)] + \varepsilon^f[\mathbf{p} + \mathbf{q}' - e\mathbf{A}(T)]\}\langle f_{\mathbf{p}+\mathbf{q}+\mathbf{q}'}^\dagger f_{\mathbf{p}}c_{\mathbf{k}-\mathbf{q}}^\dagger c_{\mathbf{k}+\mathbf{q}'}\rangle(T) + U^2\sum_{\mathbf{p},\mathbf{p}',\mathbf{q}}\{\varepsilon[\mathbf{k} + \mathbf{q} - e\mathbf{A}(T)] - \varepsilon[\mathbf{k} - e\mathbf{A}(T)]$$
$$+ \varepsilon^f[\mathbf{p}' - e\mathbf{A}(T)] - \varepsilon^f[\mathbf{p}' - \mathbf{q} - e\mathbf{A}(T)] + 2\varepsilon^f[\mathbf{p} - e\mathbf{A}(T)] - 2\varepsilon^f[\mathbf{p} + \mathbf{q} - e\mathbf{A}(T)]\}\langle f_{\mathbf{p}'-\mathbf{q}}^\dagger f_{\mathbf{p}'}f_{\mathbf{p}+\mathbf{q}}^\dagger f_{\mathbf{p}}\rangle(T) + U^3n_f. \quad (25)$$

Summing over momentum yields the following local moments:

$$\mu_0^R(T) = 1, \quad (26)$$

$$\mu_1^R(T) = -\mu + Un_f, \quad (27)$$

$$\mu_2^R(T) = \frac{t^{*2}}{2} + \mu^2 - 2U\mu n_f + U^2n_f, \quad (28)$$

$$\mu_3^R(T) = -\frac{3t^{*2}}{2}(\mu - Un_f) + 3U\mu n_f(\mu - Un_f)$$
$$+ 3U^2\mu n_f(n_f - 1) + U^3 n_f - \mu^3 + 2U^2\sum_{ij}\tilde{t}_{ij}^f\langle f_i^\dagger f_j\rangle$$
$$- 2U^2\sum_{ij}\tilde{t}_{ij}^f(\langle f_i^\dagger f_j c_j^\dagger c_i\rangle + \langle f_i^\dagger f_j c_i^\dagger c_i\rangle)$$
$$+ U^2\sum_{ij}\tilde{t}_{ij}^f(-\langle f_i^\dagger f_j f_i^\dagger f_i\rangle + \langle f_i^\dagger f_j f_j^\dagger f_j\rangle - 2\langle f_i^\dagger f_i f_i^\dagger f_j\rangle$$
$$+ 2\langle f_j^\dagger f_j f_i^\dagger f_j\rangle), \tag{29}$$

where $\tilde{t}_{ij}^f$ is defined in Eq. (3). In these equations, we have assumed that we are on the infinite-dimensional hypercubic lattice and have explicitly evaluated the second moment of the hopping matrix; the generalization to finite dimensions is simple to complete (see the erratum of Ref. 17).

As follows from Eqs. (26)–(28), the zeroth and the first two retarded moments remain time independent even in the case of an arbitrary external time-dependent field. The third local moment [in Eq. (29)] is time independent for the case of the Falicov–Kimball model ($\tilde{t}^f = 0$). In the case of the Hubbard model, its expression is complex and we cannot immediately tell whether they are time dependent (but they most likely are). The last two terms in Eq. (29) are defined by electron correlations and they define the shape of the spectral functions of the lower and upper Hubbard bands, the redistribution of the spectral weights between the bands, and a shift of their centers of gravity.[28,29] It is difficult to obtain analytical expressions for these terms.

In a similar way, one can obtain expressions for the lesser moments from Eqs. (18)–(21),

$$\mu_0^<(\mathbf{k}, T) = 2\langle n_k(T)\rangle, \tag{30}$$

$$\mu_1^<(\mathbf{k}, T) = 2\{\varepsilon[\mathbf{k} - e\mathbf{A}(T)] - \mu\}\langle n_\mathbf{k}(T)\rangle$$
$$+ U\sum_{\mathbf{p,q}}[\langle c_\mathbf{k}^\dagger c_{\mathbf{k+q}}f_{\mathbf{p+q}}^\dagger f_\mathbf{p}\rangle(T) + \langle c_{\mathbf{k-q}}^\dagger c_\mathbf{k}f_{\mathbf{p+q}}^\dagger f_\mathbf{p}\rangle(T)], \tag{31}$$

$$\mu_2^<(\mathbf{k}, T) = 2\{\varepsilon[\mathbf{k} - e\mathbf{A}(T)] - \mu\}^2\langle n_\mathbf{k}(T)\rangle + \frac{3}{2}U\{\varepsilon[\mathbf{k} - e\mathbf{A}(T)] - \mu\}\sum_{\mathbf{p,q}}[\langle f_{\mathbf{p+q}}^\dagger f_\mathbf{p}c_{\mathbf{k-q}}^\dagger c_\mathbf{k}\rangle(T) + \langle f_{\mathbf{p+q}}^\dagger f_\mathbf{p}c_\mathbf{k}^\dagger c_{\mathbf{k+q}}\rangle]$$
$$+ \frac{1}{2}U\sum_{\mathbf{p,q}}\{\varepsilon[\mathbf{k} - \mathbf{q} - e\mathbf{A}(T)] - \mu\}\langle f_{\mathbf{p+q}}^\dagger f_\mathbf{p}c_{\mathbf{k-q}}^\dagger c_\mathbf{k}\rangle(T) + \frac{1}{2}U\sum_{p,q}\{\varepsilon[\mathbf{k} + \mathbf{q} - e\mathbf{A}(T)] - \mu\}\langle f_{\mathbf{p+q}}^\dagger f_\mathbf{p}c_\mathbf{k}^\dagger c_{\mathbf{k+q}}\rangle(T)$$
$$- \frac{1}{2}U\sum_{\mathbf{p,q}}\{\varepsilon^f[\mathbf{p} + \mathbf{q} - e\mathbf{A}(T)] - \varepsilon^f[\mathbf{p} - e\mathbf{A}(T)]\}[\langle f_{\mathbf{p+q}}^\dagger f_\mathbf{p}c_\mathbf{k}^\dagger c_{\mathbf{k+q}}\rangle(T) - \langle f_{\mathbf{p+q}}^\dagger f_\mathbf{p}c_{\mathbf{k-q}}^\dagger c_\mathbf{k}\rangle(T)]$$
$$+ \frac{1}{2}U^2\sum_{\mathbf{p,q,P,Q}}[\langle f_{\mathbf{p+q}}^\dagger f_\mathbf{p}f_{\mathbf{P+Q}}^\dagger f_\mathbf{P}c_{\mathbf{k-q-Q}}^\dagger c_\mathbf{k}\rangle(T) + 2\langle f_{\mathbf{p+q}}^\dagger f_\mathbf{p}f_{\mathbf{P+Q}}^\dagger f_\mathbf{P}c_{\mathbf{k-q}}^\dagger c_{\mathbf{k+Q}}\rangle(T) + \langle f_{\mathbf{p+q}}^\dagger f_\mathbf{p}f_{\mathbf{P+Q}}^\dagger f_\mathbf{P}c_\mathbf{k}^\dagger c_{\mathbf{k+Q+q}}\rangle(T)], \tag{32}$$

$$\mu_3^<(\mathbf{k}, T) = 2\{\varepsilon[\mathbf{k} - e\mathbf{A}(T)] - \mu\}^3\langle c_\mathbf{k}^\dagger c_\mathbf{k}\rangle(T) + 2U\{\varepsilon[\mathbf{k} - e\mathbf{A}(T)] - \mu\}^2\sum_{\mathbf{p,q}}\langle c_\mathbf{k}^\dagger c_{\mathbf{k+q}}f_{\mathbf{p+q}}^\dagger f_\mathbf{p}\rangle(T) + 2U\sum_{\mathbf{p',p}}\{\varepsilon[\mathbf{k} - e\mathbf{A}(T)] + \varepsilon[\mathbf{p}$$
$$- e\mathbf{A}(T)] - 2\mu + \varepsilon^f[\mathbf{p'} - e\mathbf{A}(T)] - \varepsilon^f[\mathbf{p'} + \mathbf{p} - \mathbf{k} - e\mathbf{A}(T)]\}\{\varepsilon[\mathbf{p} - e\mathbf{A}(T)] - \mu\}\langle c_\mathbf{k}^\dagger c_\mathbf{p}f_{\mathbf{p'+p-k}}^\dagger f_{\mathbf{p'}}\rangle(T)$$
$$+ 2U\sum_{\mathbf{q',p}}\{\varepsilon[\mathbf{k} - e\mathbf{A}(T)] + \varepsilon[\mathbf{k} + \mathbf{q'} - e\mathbf{A}(T)] - 2\mu + \varepsilon^f[\mathbf{p} - e\mathbf{A}(T)] - \varepsilon^f[\mathbf{p} + \mathbf{q'} - e\mathbf{A}(T)]\}\{\varepsilon^f[\mathbf{p} - e\mathbf{A}(T)]$$
$$- \varepsilon^f[\mathbf{p} + \mathbf{q'} - e\mathbf{A}(T)]\}\langle c_\mathbf{k}^\dagger c_{\mathbf{k+q'}}f_{\mathbf{p+q'}}^\dagger f_\mathbf{p}\rangle(T) + 2U^2\sum_{\mathbf{p',q',p,q}}\{\varepsilon[\mathbf{k} - e\mathbf{A}(T)] + \varepsilon[\mathbf{k} + \mathbf{q'} - e\mathbf{A}(T)] - 2\mu + \varepsilon^f[\mathbf{p'} - e\mathbf{A}(T)]$$
$$- \varepsilon^f[\mathbf{p'} + \mathbf{q'} - e\mathbf{A}(T)]\}\langle f_{\mathbf{p+q}}^\dagger f_\mathbf{p}f_{\mathbf{p'+q'}}^\dagger f_{\mathbf{p'}}c_\mathbf{k}^\dagger c_{\mathbf{k+q'+q}}\rangle(T) + 2U^2\sum_{\mathbf{q',p,q,k'}}\{\varepsilon^f[\mathbf{p} + \mathbf{q} - e\mathbf{A}(T)] - \varepsilon^f[\mathbf{p} + \mathbf{q} + \mathbf{q'} - e\mathbf{A}(T)]$$
$$- \varepsilon^f[\mathbf{p} - e\mathbf{A}(T)] + \varepsilon^f[\mathbf{p} + \mathbf{q'} - e\mathbf{A}(T)]\}\langle f_{\mathbf{p+q+q'}}^\dagger f_\mathbf{p}c_\mathbf{k}^\dagger c_{\mathbf{k+q'}}c_{\mathbf{k'-q}}^\dagger c_{\mathbf{k'}}\rangle(T) + 2U^2\sum_{\mathbf{p',q',p,q}}\{\varepsilon[\mathbf{k} + \mathbf{q} + \mathbf{q'} - e\mathbf{A}(T)]$$
$$- \mu - \varepsilon^f[\mathbf{p'} + \mathbf{q'} - e\mathbf{A}(T)] + \varepsilon^f[\mathbf{p'} - e\mathbf{A}(T)] - \varepsilon^f[\mathbf{p} + \mathbf{q} - e\mathbf{A}(T)] + \varepsilon^f[\mathbf{p} - e\mathbf{A}(T)]\}\langle f_{\mathbf{p'+q'}}^\dagger f_{\mathbf{p'}}f_{\mathbf{p+q}}^\dagger f_\mathbf{p}c_\mathbf{k}^\dagger c_{\mathbf{k+q+q'}}\rangle(T)$$
$$+ 2U^3\sum_{\mathbf{p',q',p,q,P,Q}}\langle f_{\mathbf{P+Q}}^\dagger f_\mathbf{P}f_{\mathbf{p'+q'}}^\dagger f_{\mathbf{p'}}f_{\mathbf{p+q}}^\dagger f_\mathbf{p}c_\mathbf{k}^\dagger c_{\mathbf{Q+k+q+q'}}\rangle(T). \tag{33}$$

The corresponding local lesser moments are

$$\mu_0^<(T) = 2n_c(T), \tag{34}$$

$$\mu_1^<(T) = -2\sum_{i,j} \tilde{t}_{ij}\langle c_i^\dagger c_j\rangle - 2\mu n_c + 2U\sum_i \langle f_i^\dagger f_i c_i^\dagger c_i\rangle, \tag{35}$$

$$\mu_2^<(T) = 2\sum_{i,l,j} \tilde{t}_{il}\tilde{t}_{lj}\langle c_i^\dagger c_j\rangle + 4\mu\sum_{i,j} \tilde{t}_{ij}\langle c_i^\dagger c_j\rangle + 2\mu^2 n_c(T) - 2U\sum_{i,j}[\tilde{t}_{ij}\langle f_i^\dagger f_i c_i^\dagger c_j\rangle + \tilde{t}_{ji}\langle f_i^\dagger f_i c_j^\dagger c_i\rangle] + 2U(U-2\mu)\sum_i \langle f_i^\dagger f_i c_i^\dagger c_i\rangle, \tag{36}$$

$$\begin{aligned}
\mu_3^<(T) = &-2\sum_{i,j,l,m} \tilde{t}_{il}\tilde{t}_{lm}\tilde{t}_{mj}\langle c_i^\dagger c_j\rangle(T) - 6\mu\sum_{i,j,l} \tilde{t}_{il}\tilde{t}_{lj}\langle c_i^\dagger c_j\rangle(T) - 6\mu^2\sum_{i,j} \tilde{t}_{ij}\langle c_i^\dagger c_j\rangle(T) - 2\mu^3\sum_i \langle c_i^\dagger c_i\rangle(T) + 2U\sum_{i,l,j} \tilde{t}_{il}\tilde{t}_{lj}\langle c_i^\dagger c_j f_j^\dagger f_j\rangle(T) \\
&+ 2(3U\mu^2 - 3U^2\mu + U^3)\sum_i \langle f_i^\dagger f_i c_i^\dagger c_i\rangle(T) + 6U\mu\sum_{i,j} \tilde{t}_{ij}\langle c_i^\dagger c_j f_j^\dagger f_j\rangle(T) + 6U\mu\sum_{i,j} \tilde{t}_{ij}\langle c_i^\dagger c_j f_i^\dagger f_i\rangle(T) - 2U^2\sum_{i,j} \tilde{t}_{ij}\langle f_j^\dagger f_j c_i^\dagger c_j\rangle(T) \\
&- 2U^2\sum_{i,j} \tilde{t}_{ij}\langle f_i^\dagger f_i c_i^\dagger c_j\rangle(T) + 2U\sum_{i,l,j} \tilde{t}_{il}\tilde{t}_{lj}\langle c_i^\dagger c_l f_j^\dagger f_j\rangle(T) + 2U\sum_{i,l,j} \tilde{t}_{il}\tilde{t}_{lj}\langle c_i^\dagger c_j f_i^\dagger f_i\rangle(T) - 2U^2\sum_{i,j} \tilde{t}_{ij}\langle f_j^\dagger f_j f_i^\dagger f_i c_i^\dagger c_j\rangle(T) \\
&+ 2U\sum_{i,j,l} \tilde{t}_{ij}\tilde{t}_{il}^f\langle c_i^\dagger c_j f_i^\dagger f_l\rangle(T) - 2U\sum_{i,j,l} \tilde{t}_{ij}\tilde{t}_{li}^f\langle c_i^\dagger c_j f_l^\dagger f_i\rangle(T) + 2U\mu\sum_{i,j} \tilde{t}_{ij}^f\langle c_i^\dagger c_i f_i^\dagger f_j\rangle(T) - 2U\mu\sum_{i,j} \tilde{t}_{ji}^f\langle c_i^\dagger c_i f_j^\dagger f_i\rangle(T) \\
&+ 2U\sum_{i,j,l} \tilde{t}_{il}^f\tilde{t}_{lj}^f\langle c_i^\dagger c_i f_i^\dagger f_j\rangle(T) + 2U\sum_{i,j,l} \tilde{t}_{il}^f\tilde{t}_{lj}^f\langle c_i^\dagger c_j f_i^\dagger f_j\rangle(T) - 4U\sum_{i,j,l} \tilde{t}_{ji}^f\tilde{t}_{il}^f\langle c_i^\dagger c_i f_j^\dagger f_l\rangle(T) - 2U^2\sum_{i,j} \tilde{t}_{ij}^f[\langle f_i^\dagger f_i f_j^\dagger f_j c_i^\dagger c_i\rangle(T) \\
&- \langle f_j^\dagger f_j f_i^\dagger f_i c_j^\dagger c_j\rangle(T)] - 4U^2\sum_{i,j} \tilde{t}_{ij}\langle f_i^\dagger f_j c_i^\dagger c_i c_j^\dagger c_j\rangle(T) + 4U^2\sum_{i,j} \tilde{t}_{ij}^f\langle f_i^\dagger f_j c_j^\dagger c_j\rangle(T), \tag{37}
\end{aligned}$$

where $\tilde{t}_{ij}$ is defined in Eq. (2).

Contrary to the case of the retarded moments, even the zeroth and the first two local lesser moments in Eqs. (34)–(36) cannot be solely expressed in terms of the model parameters, and they depend on different correlation functions. Therefore, in order to check the accuracy of calculations in the lesser case, one can only compare the numerical results for the lesser moments obtained by direct calculations by using Eq. (11) with the corresponding results obtained by a numerical evaluation of the time derivatives of the Green function in Eq. (12). However, the results in Eqs. (34)–(37) still contain practical importance because they provide a simple way to calculate combinations of different correlation functions. The reason for this is due to the fact that the correlation functions on the right hand side of Eqs. (34)–(37) can be expressed in terms of the local lesser Green functions and their time derivatives by using Eq. (12), the equation of motion, and/or the Dyson equations for the Green functions [see Eqs. (39) and (44)–(46), below]. For example, as shown in Ref. 17, we can connect the average potential energy (evaluated at average time $T = t_1$) with the Green functions and self-energies,

$$\begin{aligned}
U\langle f_i^\dagger f_i c_i^\dagger c_i\rangle = &-i\sum_{\mathbf{k}}\left\{i\frac{\partial}{\partial t_1} + \mu - \epsilon\left[\mathbf{k}\right.\right. \\
&\left.\left. - \frac{e\mathbf{A}(t_1)}{\hbar c}\right]\right\}G_{\mathbf{k}}^<(t_1,t_2)\bigg|_{t_2=t_1} \\
= &-i\sum_{\mathbf{k}}\int dt[\Sigma_{\mathbf{k}}^R(t_1,t)G_{\mathbf{k}}^<(t,t_1) + \Sigma_{\mathbf{k}}^<(t_1,t)G_{\mathbf{k}}^A(t,t_1)],
\end{aligned}$$

$$\tag{38}$$

a generalization of the well-known equilibrium result.

IV. SPECTRAL MOMENTS FOR THE RETARDED SELF-ENERGY

It is possible to derive expressions for the lowest retarded self-energy moments by using the Dyson equation, which connects the retarded Green function and self-energy, and the results for the retarded Green function moments derived in the previous section.

In order to derive the nonequilibrium Dyson equation for the retarded Green function, it is convenient to write down the Dyson equation for the contour-ordered lattice Green function in the Larkin–Ovchinnikov representation, where all the time arguments are defined on the real branch of the time contour,

$$\begin{aligned}
\hat{G}_{\mathbf{k}}(t_1,t_2) = &\hat{G}_{\mathbf{k}}^0(t_1,t_2) \\
&+ \int_{-\infty}^\infty dt_3\int_{-\infty}^\infty dt_4\hat{G}_{\mathbf{k}}^0(t_1,t_3)\hat{\Sigma}_{\mathbf{k}}(t_3,t_4)\hat{G}_{\mathbf{k}}(t_4,t_2),
\end{aligned}$$

$$\tag{39}$$

and all the Green functions and self-energy functions are 2×2 matrices,

$$\hat{G}_{\mathbf{k}}(t_1,t_2) = \begin{pmatrix} G_{\mathbf{k}}^R(t_1,t_2) & G_{\mathbf{k}}^K(t_1,t_2) \\ 0 & G_{\mathbf{k}}^A(t_1,t_2) \end{pmatrix}, \tag{40}$$

$$\hat{\Sigma}_{\mathbf{k}}(t_1,t_2) = \begin{pmatrix} \Sigma_{\mathbf{k}}^R(t_1,t_2) & \Sigma_{\mathbf{k}}^K(t_1,t_2) \\ 0 & \Sigma_{\mathbf{k}}^A(t_1,t_2) \end{pmatrix}, \tag{41}$$

with matrix elements consisting of the retarded, advanced

$$G_{\mathbf{k}}^A(t_1,t_2) = i\,\theta(t_2 - t_1)\langle[c_{\mathbf{k}H}(t_1), c_{\mathbf{k}H}^{\dagger}(t_2)]\rangle, \qquad (42)$$

and the Keldysh

$$G_{\mathbf{k}}^K(t_1,t_2) = -i\langle[c_{\mathbf{k}H}(t_1), c_{\mathbf{k}H}^{\dagger}(t_2)]\rangle \qquad (43)$$

components (and similarly for the self-energy). The function $\hat{G}_{\mathbf{k}}^{(0)}$ in Eq. (39) is the electron Green function in the noninteracting case ($U=0$ but with $E \neq 0$ for the nonequilibrium case). The expression for this function can be analytically obtained (see, for example, Refs. 34 and 35).

The nonzero matrix components of the Dyson equation can be written in the following form:

$$G_{\mathbf{k}}^R(t_1,t_2) = G_{\mathbf{k}}^{R0}(t_1,t_2) + [G_{\mathbf{k}}^{R0}\Sigma_{\mathbf{k}}^R G_{\mathbf{k}}^R](t_1,t_2), \qquad (44)$$

$$G_{\mathbf{k}}^A(t_1,t_2) = G_{\mathbf{k}}^{A0}(t_1,t_2) + [G_{\mathbf{k}}^{A0}\Sigma_{\mathbf{k}}^A G_{\mathbf{k}}^A](t_1,t_2), \qquad (45)$$

$$G_{\mathbf{k}}^K(t_1,t_2) = [1 + G_{\mathbf{k}}^R\Sigma_{\mathbf{k}}^R]G_{\mathbf{k}}^{K0}[1 + \Sigma_{\mathbf{k}}^A G_{\mathbf{k}}^A](t_1,t_2)$$
$$+ [G_{\mathbf{k}}^R\Sigma_{\mathbf{k}}^K G_{\mathbf{k}}^A](t_1,t_2), \qquad (46)$$

where we suppressed integrations over internal time variables implied by the continuous matrix operator multiplications.

In order to find the retarded self-energy spectral moments, one only needs Eq. (44). It is convenient to rewrite this equation in a combined frequency-average time representation,

$$G_{\mathbf{k}}^R(T,\omega) = G_{\mathbf{k}}^{R0}(T,\omega) + \int d\bar{T} \int d\bar{t} \int d\Omega \int d\nu\, e^{-i\Omega\bar{t}} e^{i\nu\bar{T}}$$
$$\times G_{\mathbf{k}}^{R0}\left(T + \frac{\bar{T}}{2} + \frac{\bar{t}}{4}, \omega + \Omega + \frac{\nu}{2}\right)\Sigma_{\mathbf{k}}^R(T + \bar{T}, \omega + 2\Omega)$$
$$\times G_{\mathbf{k}}^R\left(T + \frac{\bar{T}}{2} - \frac{\bar{t}}{4}, \omega + \Omega - \frac{\nu}{2}\right), \qquad (47)$$

where we restored the internal time-frequency integrations.

Similar to the equilibrium case,[28,29,31] one can expand the Green functions and the self-energies at large values of the frequency ω in terms of the corresponding moments,

$$G_{\mathbf{k}}^R(T,\omega) = \sum_{m=0}^{\infty} \frac{\mu_m^R(\mathbf{k},T)}{\omega^{m+1}}, \qquad (48)$$

$$\Sigma_{\mathbf{k}}^R(T,\omega) = \Sigma_{\mathbf{k}}^R(T,\omega=\infty) + \sum_{m=0}^{\infty} \frac{C_m^R(\mathbf{k},T)}{\omega^{m+1}}, \qquad (49)$$

where the moments $\mu_m^R(\mathbf{k},T)$ and $C_m^R(\mathbf{k},T)$ correspond to the retarded Green function and self-energy in Eq. (44). In particular, we have

$$C_m^R(\mathbf{k},T) = -\frac{1}{\pi}\,\mathrm{Im}\int_{-\infty}^{\infty} dt\, e^{i\omega t}\omega^m\Sigma_{\mathbf{k}}^R(T,t). \qquad (50)$$

The large-ω expansions in Eqs. (48) and (49) can be obtained by using the following spectral identities (valid for retarded functions that rapidly decay enough for large relative time):

$$G_{\mathbf{k}}^R(T,\omega) = -\frac{1}{\pi}\int_{-\infty}^{\infty} d\omega'\frac{\mathrm{Im}\,G_{\mathbf{k}}^R(T,\omega')}{\omega - \omega'}, \qquad (51)$$

$$\Sigma_{\mathbf{k}}^R(T,\omega) = -\frac{1}{\pi}\int_{-\infty}^{\infty} d\omega'\frac{\mathrm{Im}\,\Sigma_{\mathbf{k}}^R(T,\omega')}{\omega - \omega'} + \Sigma_{\mathbf{k}}^R(T,\omega=\infty), \qquad (52)$$

where we take ω large enough that the Green function and self-energy on the left hand side are real. In fact, by making expansions in powers of $(1/\omega)$ on the right hand sides of Eqs. (51) and (52) and by using the moment definitions in Eqs. (11) and (12), one can obtain the expansions in Eqs. (48) and (49). The self-energy expansion in Eq. (49) contains a frequency-independent term $\Sigma_{\mathbf{k}}^R(T,\omega=\infty)$, which corresponds to the mean-field term of the self-energy [see Eq. (58) below]; this form arises because the self-energy generically approaches a real constant nonzero value as $|\omega| \to \infty$.

Then, one can insert these expansions into Eq. (47) and separately consider the terms that have the same order in $(1/\omega)$. In order to do this, it is necessary to expand all the functions under the integrals in powers of $(1/\omega)$. For example,

$$G_{\mathbf{k}}^R\left(T + \frac{\bar{T}}{2} - \frac{\bar{t}}{4}, \omega + \Omega - \frac{\nu}{2}\right) = \sum_{m=0}^{\infty} \frac{\mu_m^R\left(\mathbf{k}, T + \frac{\bar{T}}{2} - \frac{\bar{t}}{4}\right)}{\left(\omega + \Omega - \frac{\nu}{2}\right)^{m+1}}$$
$$= \sum_{m=0}^{\infty} \frac{\mu_m^R\left(\mathbf{k}, T + \frac{\bar{T}}{2} - \frac{\bar{t}}{4}\right)}{\omega^{m+1}}$$
$$\times \frac{1}{\left[1 + \left(\Omega - \frac{\nu}{2}\right)/\omega\right]^{m+1}}$$
$$= \sum_{m=0}^{\infty} \frac{\mu_m^R\left(\mathbf{k}, T + \frac{\bar{T}}{2} - \frac{\bar{t}}{4}\right)}{\omega^{m+1}}$$
$$\times \left(1 - \frac{\Omega - \frac{\nu}{2}}{\omega} + \cdots\right)^{m+1}. \qquad (53)$$

To calculate the frequency-independent term and the zeroth and the first spectral moments for the retarded self-energy, it is necessary to make an expansion of the functions in powers of $1/\omega$ in Eq. (47) up to fourth order. All the time and frequency integrals in Eq. (47) can be easily performed, and we get the following equations that connect the Green functions and self-energy spectral moments:

$$\mu_0^R(\mathbf{k},T) = \tilde{\mu}_0^R(\mathbf{k},T), \qquad (54)$$

$$\mu_1^R(\mathbf{k},T) = \tilde{\mu}_1^R(\mathbf{k},T) + \tilde{\mu}_0^R(\mathbf{k},T)\Sigma_{\mathbf{k}}^R(T,\omega=\infty)\mu_0^R(\mathbf{k},T), \qquad (55)$$

$$\mu_2^R(\mathbf{k},T) = \tilde{\mu}_2^R(\mathbf{k},T) + \tilde{\mu}_0^R(\mathbf{k},T)\Sigma_{\mathbf{k}}^R(T,\omega=\infty)\mu_1^R(\mathbf{k},T)$$
$$+ \tilde{\mu}_0^R(\mathbf{k},T)C_0^R(\mathbf{k},T)\mu_0^R(\mathbf{k},T)$$
$$+ \tilde{\mu}_1^R(\mathbf{k},T)\Sigma_{\mathbf{k}}^R(T,\omega=\infty)\mu_0^R(\mathbf{k},T), \quad (56)$$

$$\mu_3^R(\mathbf{k},T) = \tilde{\mu}_3^R(\mathbf{k},T) + \tilde{\mu}_0^R(\mathbf{k},T)\Sigma_{\mathbf{k}}^R(T,\omega=\infty)\mu_2^R(\mathbf{k},T)$$
$$+ \tilde{\mu}_0^R(\mathbf{k},T)C_0^R(\mathbf{k},T)\mu_1^R(\mathbf{k},T)$$
$$+ \tilde{\mu}_0^R(\mathbf{k},T)C_1^R(\mathbf{k},T)\mu_0^R(\mathbf{k},T)$$
$$+ \tilde{\mu}_1^R(\mathbf{k},T)\Sigma_{\mathbf{k}}^R(T,\omega=\infty)\mu_1^R(\mathbf{k},T)$$
$$+ \tilde{\mu}_1^R(\mathbf{k},T)C_0^R(\mathbf{k},T)\mu_0^R(\mathbf{k},T)$$

$$+ \tilde{\mu}_2^R(\mathbf{k},T)\Sigma_{\mathbf{k}}^R(T,\omega=\infty)\mu_0^R(\mathbf{k},T), \quad (57)$$

where the matrix $\tilde{\mu}_n^R(\mathbf{k},T)$ is the nth spectral moment of the retarded Green function in the *noninteracting case*. One can straightforwardly derive expressions for the retarded self-energy moments from Eqs. (54)–(57) by using the results in Eqs. (24) and (25) for the retarded Green function moments. After some long algebra, we find

$$\Sigma_{\mathbf{k}}^R(T,\omega=\infty) = Un_f, \quad (58)$$

$$C_0^R(\mathbf{k},T) = n_f(1-n_f)U^2, \quad (59)$$

$$C_1^R(\mathbf{k},T) = U^2 n_f(1-n_f)[U(1-n_f)-\mu] + U^2\sum_{\mathbf{p},\mathbf{q}}\{\varepsilon^f[\mathbf{p}+\mathbf{q}-e\mathbf{A}(T)]-2\varepsilon^f[\mathbf{p}-e\mathbf{A}(T)]$$
$$+\varepsilon^f[\mathbf{p}-\mathbf{q}-e\mathbf{A}(T)]\}\langle f_{\mathbf{p}}^\dagger f_{\mathbf{p}}\rangle(T) - U^2\sum_{\mathbf{p},\mathbf{q},\mathbf{q}'}\{\varepsilon^f[\mathbf{p}+\mathbf{q}-e\mathbf{A}(T)]-\varepsilon^f[\mathbf{p}+\mathbf{q}+\mathbf{q}'-e\mathbf{A}(T)]$$
$$-\varepsilon^f[\mathbf{p}-e\mathbf{A}(T)]+\varepsilon^f[\mathbf{p}+\mathbf{q}'-e\mathbf{A}(T)]\}\langle f_{\mathbf{p}+\mathbf{q}+\mathbf{q}'}^\dagger f_{\mathbf{p}}c_{\mathbf{k}-\mathbf{q}}^\dagger c_{\mathbf{k}+\mathbf{q}'}\rangle(T) + U^2\sum_{\mathbf{p},\mathbf{p}',\mathbf{q}}\{\varepsilon[\mathbf{k}+\mathbf{q}-e\mathbf{A}(T)]-\varepsilon[\mathbf{k}-e\mathbf{A}(T)]$$
$$+\varepsilon^f[\mathbf{p}'-e\mathbf{A}(T)]-\varepsilon^f[\mathbf{p}'-\mathbf{q}-e\mathbf{A}(T)]+2\varepsilon^f[\mathbf{p}-eA(T)]-2\varepsilon^f[\mathbf{p}+\mathbf{q}-e\mathbf{A}(T)]\}\langle f_{\mathbf{p}'-\mathbf{q}}^\dagger f_{\mathbf{p}'}f_{\mathbf{p}+\mathbf{q}}^\dagger f_{\mathbf{p}}\rangle(T). \quad (60)$$

The expressions for the local moments are

$$C_0^R(T) = n_f(1-n_f)U^2, \quad (61)$$

$$C_1^R(T) = U^2 n_f(1-n_f)[U(1-n_f)-\mu] + 2U^2\sum_{ij}\tilde{t}_{ij}^f\langle f_i^\dagger f_j\rangle$$
$$- U^2\sum_{ij}\tilde{t}_{ij}^f(\langle f_i^\dagger f_j c_j^\dagger c_i\rangle + \langle f_i^\dagger f_j c_i^\dagger c_i\rangle)$$
$$+ U^2\sum_{ij}\tilde{t}_{ij}^f(-\langle f_i^\dagger f_j f_i^\dagger f_i\rangle + \langle f_i^\dagger f_j f_j^\dagger f_j\rangle$$
$$- 2\langle f_i^\dagger f_i f_i^\dagger f_j\rangle + 2\langle f_j^\dagger f_j f_i^\dagger f_j\rangle). \quad (62)$$

It is worthwhile to notice that the local retarded self-energy moments are time independent (except for the first moment in the case of the Hubbard model, for which we are not sure about the time dependence). This may be a surprising result for the Hubbard model since the second-order perturbation theory is frequency dependent, but the total weight of the self-energy remains constant and depends just on the electron densities and the interaction. Other interesting observations are that the mean-field term $\Sigma_{\mathbf{k}}^R(T,\omega=\infty)$ is equal to the first order (Hartree–Fock) term of the self-energy in the expansion in U and that the zeroth moment corresponds to the zeroth moment of the imaginary part of $\Sigma^R(\omega,T)$ in the truncated second-order perturbation expansion[15] (for the Falicov–Kimball model case). This is in agreement with the result of Ref. 36, where it was shown that in equilibrium, the exact coefficient of the term proportional to $1/\omega_n$ in the large

Matsubara frequency expansion of the electron self-energy of the Hubbard model can be obtained from the second-order skeleton diagram for the exact Green function. Finally, it was shown in Ref. 37, in the insulating phase, that the imaginary part of the $d\to\infty$ equilibrium retarded self-energy acquires an additional term proportional to $\delta(\omega)$ in the frequency representation (at half-filling, away from half-filling, a delta function appears but not at $\omega=0$). In particular, in the case of the Falicov–Kimball model, the weight of the delta-function term is equal to $-\pi[U^2 n_f(1-n_f)-1/2]$ and it produces a term that requires special care to include in the zeroth self-energy moment when one performs the integration over frequency of the self-energy. Note that the delta function implies that the finite-frequency integration of the zeroth self-energy moment remains fixed at 0.5 for the Falicov–Kimball model in the insulating phase at half-filling, and all of the additional spectral weight comes from the delta-function piece at $\omega=0$. Away from half-filling, the delta function typically contributes to all moments because it appears at a finite frequency. In the nonequilibrium case, the situation is more complicated because we cannot prove that such a term is also present in this case. To see whether such a term is present, one needs to examine the large relative-time limit of the nonequilibrium retarded self-energy, which would have a constant term equal to the weight of the delta function when the delta function appears at $\omega=0$ (and would be a term proportional to $\exp(i\omega t)$ when the delta function is at a finite frequency), but we do find good overall agreement for the sum rules, so this issue is not important in verifying the

accuracy (when one performs calculations in the time representation).

Unfortunately, it is impossible to derive analogous expressions for the lesser self-energy spectral moments,

$$C_m^<(\mathbf{k},T) = \frac{1}{\pi}\int_{-\infty}^{\infty} d\omega \omega^m \, \mathrm{Im}\, \Sigma_\mathbf{k}^<(T,\omega), \qquad (63)$$

since in this case the expansions similar to Eqs. (48) and (49) do not exist. In fact, the representations in Eqs. (51) and (52), which lead to Eqs. (48) and (49), are not valid in the cases of the lesser Green function and self-energy because the lesser functions are pure imaginary and, hence, not analytic. Note that we could try to define an auxiliary Green function that has the imaginary part of the lesser Green function and a real part determined by a Kramers–Kronig relation, but doing so does not produce any new results for the spectral moments of the lesser self-energy.

An alternate approach is to express the lesser self-energy in terms of the retarded Green function and self-energy by using the system of Dyson equations in Eqs. (44)–(46) and the equation that connects the lesser Green function with the retarded, advanced, and Keldysh Green functions,

$$G_\mathbf{k}^<(t_1,t_2) = \frac{1}{2}[G_\mathbf{k}^K(t_1,t_2) - G_\mathbf{k}^R(t_1,t_2) + G_\mathbf{k}^A(t_1,t_2)], \quad (64)$$

and then try to express the lesser self-energy moments in terms of moments for the retarded and lesser Green functions and the retarded self-energy. In this case, one can find the following Dyson equation for the lesser self-energy:

$$G_\mathbf{k}^<(t_1,t_2) = [1 + G_\mathbf{k}^R\Sigma_\mathbf{k}^R]G_\mathbf{k}^{<0}[1 + \Sigma_\mathbf{k}^A G_\mathbf{k}^A](t_1,t_2)$$
$$+ [G_\mathbf{k}^R\Sigma_\mathbf{k}^< G_\mathbf{k}^A](t_1,t_2). \qquad (65)$$

By using the equations of motion for the Green functions (with an implicit integration over the internal time variables):

$$\left(\delta(t-t_1)\left\{i\frac{\partial}{\partial t_1} - \varepsilon[\mathbf{k}-\mathbf{A}(t_1)] + \mu\right\} - \Sigma_\mathbf{k}^R(t,t_1)\right)G_\mathbf{k}^R(t_1,t_2)$$
$$= \delta(t-t_2), \qquad (66)$$

$$G_\mathbf{k}^A(t_1,t_2)\left(\left\{i\frac{\bar{\partial}}{\partial t_2} + \varepsilon[\mathbf{k}-\mathbf{A}(t_2)] - \mu\right\}\delta(t_2-t') + \Sigma_\mathbf{k}^A(t_2,t')\right)$$
$$= -\delta(t_1-t'), \qquad (67)$$

$$\left(\delta(t-t_1)\left\{i\frac{\partial}{\partial t_1} - \varepsilon[\mathbf{k}-\mathbf{A}(t_1)] - \mu\right\} - \Sigma_\mathbf{k}^<(t,t_1)\right)G_\mathbf{k}^<(t_1,t_2) = 0, \qquad (68)$$

one can get the following formal expression for the lesser self-energy:

$$\Sigma_\mathbf{k}^<(t_1,t_2) = -\left(\delta(t_1-t)\left\{i\frac{\partial}{\partial t} - \varepsilon[\mathbf{k}-\mathbf{A}(t)] + \mu\right\}\right.$$
$$\left. - \Sigma_\mathbf{k}^R(t_1,t)\right)G_\mathbf{k}^<(t,t')\left(\left\{i\frac{\bar{\partial}}{\partial t'} + \varepsilon[\mathbf{k}-\mathbf{A}(t')]\right.\right.$$
$$\left.\left. - \mu\right\}\delta(t'-t_2) + \Sigma_\mathbf{k}^A(t',t_2)\right). \qquad (69)$$

By using this result, one can calculate the lesser self-energy moments similar to what was done for the Green functions,

$$C_n^<(k,T) = \frac{1}{\pi}\, \mathrm{Im}\left[\frac{1}{(-i)^n}\frac{\partial^n}{\partial t^n}\Sigma_\mathbf{k}^<(T,t)\right]_{t=0^+}, \qquad (70)$$

where T and t are the average and the relative-time coordinates.

Unfortunately, this approach also does not provide any useful results for the self-energy moments. In fact, even in the equilibrium case, one finds from Eqs. (69) and (70) the following trivial result:

$$C_n^<(k,T) = -\frac{2}{\pi}\int d\omega \omega^n f(\omega) \mathrm{Im}\, \Sigma_\mathbf{k}^R(\omega). \qquad (71)$$

[In order to obtain this expression, one needs to use the following equilibrium relations: $\Sigma_\mathbf{k}^A(\omega) = \Sigma_\mathbf{k}^{R*}(\omega)$ and $G_\mathbf{k}^<(\omega) = -2if(\omega)\mathrm{Im}\, G_\mathbf{k}^R(\omega)$]. The result in Eq. (71) can also be directly obtained from the equilibrium relation $\Sigma_\mathbf{k}^<(\omega) = -2if(\omega)\mathrm{Im}\, \Sigma_\mathbf{k}^R(\omega)$. Unfortunately, it is impossible to get analytical results for the lesser self-energy moments from Eq. (71), except in the high-temperature limit when they can be expressed in terms of the retarded self-energy moments [via a series expansion for $f(\omega)$].

Since the exact analytical results for the lesser moments cannot be found even in the equilibrium case, one can try to make some approximations in order to obtain them. The standard approximation for the lesser Green function is the generalized Kadanoff–Baym (GKB) approximation,[38]

$$G_\mathbf{k}^<(t_1,t_2) = -i[G_\mathbf{k}^R(t_1,t_2)G_\mathbf{k}^<(t_2,t_2) - G_\mathbf{k}^<(t_1,t_1)G_\mathbf{k}^A(t_1,t_2)]. \qquad (72)$$

Substitution of this result into Eq. (69) and using the equations of motion in Eqs. (66)–(68) gives the following approximate result for the lesser self-energy,

$$\Sigma_\mathbf{k}^<(t_1,t_2) = i[\Sigma_\mathbf{k}^R(t_1,t_2)G_\mathbf{k}^<(t_2,t_2) - G_\mathbf{k}^<(t_1,t_1)\Sigma_\mathbf{k}^A(t_1,t_2)] + 2i\delta(t_1 - t_2)\frac{\partial n_\mathbf{k}(t_2)}{\partial t_2}, \qquad (73)$$

or in the frequency-average time representation,

$$\Sigma_\mathbf{k}^<(T,\omega) = -2i\, \mathrm{Im}\, \Sigma_\mathbf{k}^R(T,\omega)n_\mathbf{k}(T) + 2i\frac{\partial n_\mathbf{k}(T)}{\partial T}. \qquad (74)$$

After summation over momentum, the last term disappears, due to conservation of the total particle number; therefore, in this case,

$$C_n^<(T) = 2\sum_{\mathbf{k}} C_n^R(\mathbf{k},T) n_{\mathbf{k}}(T). \qquad (75)$$

Since the zeroth and the first retarded self-energy moments are momentum independent, one can obtain the following GKB result for the corresponding lesser moments:

$$C_n^<(T) = 2 C_n^R(T) n_c. \qquad (76)$$

The GKB approximation gives good results for the Green function moments in the case of weakly interacting systems. Therefore, the relation [Eq. (76)] should be approximately valid in this case. There is one subtle issue with regard to the GKB and DMFT. In DMFT, the self-energy is local and, hence, momentum independent. However, the GKB approximation to the self-energy in Eq. (74) appears to be momentum dependent. Hence, it is not clear how accurate the local self-energy moments will be within this approximation, but because the GKB corresponds to a mean-field-like decoupling of correlation functions for the Green function moments,[17] it is possible that the approximation remains reasonable for the local self-energy, at least for weak coupling.

Thus, generally speaking, similar to the lesser Green function moment case, one cannot obtain analytical expressions for the lesser self-energy moments. Moreover, it is even impossible to express these moments in terms of correlation functions. Hence, in order to check the accuracy of the numerical calculations, one can only compare the numerical results for the moments with the numerical evaluation of the self-energy time derivatives in Eq. (70), which is not a stringent test.

V. NUMERICAL RESULTS FOR THE FALICOV–KIMBALL MODEL IN INFINITE DIMENSIONS

In this section, we shall use results for the local moments obtained in Secs. III and IV to check the accuracy of the equilibrium and nonequilibrium numerical solutions of the Falicov–Kimball model in the limit of infinite dimensions. In this limit, the electron self-energy is local,[39] which allows one to numerically solve the problem in both equilibrium[6] and nonequilibrium cases.[16–21] The case of infinite dimensions is important since many physical properties of the model are qualitatively similar as in the two-dimensional and three-dimensional cases (see, for example, Ref. 6).

In order to study the time-dependent properties of the model in infinite dimensions, one needs to solve a generalized system of nonequilibrium DMFT equations for the contour-ordered Green function $G(t_1, t_2)$, self-energy $\Sigma(t_1, t_2)$, and an effective dynamical mean-field $\lambda(t_1, t_2)$,

$$G(t_1, t_2) = \sum_{\mathbf{k}} [G_{\mathbf{k}}^{(0)-1} - \Sigma]^{-1}(t_1, t_2), \qquad (77)$$

$$G_0(t_1, t_2) = [G^{-1} + \Sigma]^{-1}(t_1, t_2), \qquad (78)$$

$$\lambda(t_1, t_2) = G_{0imp}^{-1}(t_1, t_2; \mu) - G_0^{-1}(t_1, t_2), \qquad (79)$$
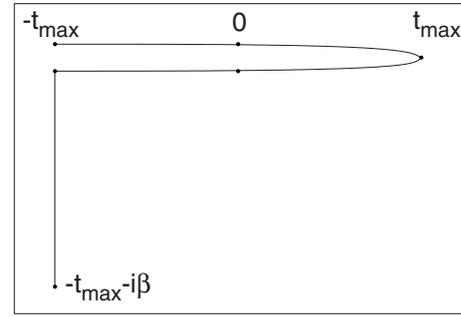
FIG. 1. The complex Kadanoff–Baym–Keldysh contour for the two-time Green functions in the nonequilibrium case.

$$G(t_1, t_2) = (1 - w_1) G_0(t_1, t_2; \mu)$$
$$+ w_1 [G_{0imp}^{-1}(\mu - U) - \lambda]^{-1}(t_1, t_2), \qquad (80)$$

where all time arguments are defined on the complex Kadanoff–Baym–Keldysh time contour (see Fig. 1). On this contour, the time increases from the top left point $(-t_{max})$ along the contour to the bottom point of the imaginary axis $(-t_{max} - i\beta)$. In Eqs. (77)–(80), $G_{\mathbf{k}}^{(0)}(t_1, t_2)$ and $G_0(t_1, t_2)$ are the noninteracting electron Green functions in the presence of an external field and the corresponding local function, defined by Eq. (78). Since in the homogeneous DMFT case the problem is translationally invariant, one can solve it by studying an effective free impurity Green function $G_{0imp}(t_1, t_2; \mu)$ for an impurity self-consistently embedded in the bath of all other electrons. The dynamical mean-field $\lambda(t_1, t_2)$ [defined in Eq. (79)] describes the effective dynamics of the impurity site with no interaction; μ is a chemical potential and w_1 is the average number of the f electrons per site (for further details, see the discussion in Refs. 20 and 21).

As mentioned in Sec. II, we shall consider the case of a spatially uniform electric field directed along the elementary cell diagonal, as in Eq. (5). We also assume that the system starts in equilibrium with an inverse temperature β, and then a constant electric field is turned on at time $t = 0$.

In the case of an external field, as given in Eq. (5), the free electron spectrum [in Eq. (7)] has a simple momentum dependence,

$$\epsilon\left[\mathbf{k} - \frac{e\mathbf{A}(t)}{\hbar c}\right] = \cos\left[\frac{eaA(t)}{\hbar c}\right] \epsilon(\mathbf{k}) + \sin\left[\frac{eaA(t)}{\hbar c}\right] \bar{\epsilon}(\mathbf{k}), \qquad (81)$$

where

$$\epsilon(\mathbf{k}) = -2t \sum_l \cos(ak^l) \qquad (82)$$

and

$$\bar{\varepsilon}(\mathbf{k}) = -2t \sum_l \sin(ak^l) \qquad (83)$$

are two energy functions. It is possible to show that in the case of an infinite-dimensional hypercubic lattice, the joint

density of states for these two energy functions has the following form:[14]

$$\rho_2(\epsilon,\bar{\epsilon}) = \frac{1}{\pi t^{*2} a^d} \exp\left[-\frac{\epsilon^2}{t^{*2}} - \frac{\bar{\epsilon}^2}{t^{*2}} \right], \quad (84)$$

where t^* is a scaled hopping parameter connected with the hopping t in the Hamiltonian [Eq. (1)] as $t = t^*/2\sqrt{d}$. The momentum summation in Eq. (77) can be performed by using the joint density of states in Eq. (84): $\Sigma_{\mathbf{k}} F_{\mathbf{k}} = \int d\epsilon \int d\bar{\epsilon} \rho_2(\epsilon,\bar{\epsilon}) F_{\epsilon,\bar{\epsilon}}$ since in our case the noninteracting Green function on the right hand side of Eq. (77) has simple momentum dependence, which can be expressed in terms of the two energy functions in Eqs. (82) and (83). The two-dimensional energy integration can be performed by using Gaussian integration.[16,18] We typically use about 100 points per dimension.

In addition, one needs to choose the proper discretization of the time contour in Fig. 1. The results strongly depend on the discretization step when the step size is not small enough. Choosing a given discretization and a t_{max} determines the matrix size for the given calculations. We typically work with general complex matrices with size of 900×900 up to 5700×5700.

A. Equilibrium case

First, we consider the equilibrium case when there is no external field. In this case the system of equations [Eqs. (77) and (80)] reduces to the equilibrium DMFT equations[40] with no average time dependence, so functions of two time arguments can be replaced by corresponding functions of one frequency, $F(t_1, t_2) \to F(\omega)$. The numerics are under good control and one can obtain quite accurate solutions. The most important numerical checks that can be performed arise from a comparison of the spectral moments directly calculated by integrating the real-frequency solutions, with results for the moments that can be exactly determined via parameters of the model for the retarded moments or by an evaluation of the relevant correlation functions using a Matsubara frequency formalism for the lesser moments.

Now, we show how to calculate the required correlation functions in Eqs. (34)–(37) using the Matsubara Green functions. One starts from the imaginary time-ordered Green functions,

$$G_{ij}(\tau) = -\langle T_\tau c_i(\tau) c_j^\dagger(0) \rangle, \quad (85)$$

where the imaginary time-dependent operators satisfy $c_i(\tau) = e^{H\tau} c_i(0) e^{-H\tau}$ according to the Heisenberg representation. Because these functions are antiperiodic on the interval $[0, \beta]$, we employ a Fourier expansion in terms of the Matsubara frequencies,

$$G_{ij}(\tau) = T \sum_{n,\mathbf{k}} e^{-i\omega_n \tau} e^{-i\mathbf{k}(\mathbf{R}_i - \mathbf{R}_j)} G_{\mathbf{k}}(i\omega_n), \quad (86)$$

where $\omega_n = \pi T(2n+1)$ is the fermionic Matsubara frequency. Here, the momentum-dependent Matsubara Green function satisfies

$$G_{\mathbf{k}}(i\omega_n) = \frac{1}{i\omega_n + \mu - \varepsilon(\mathbf{k}) - \Sigma_{\mathbf{k}}(i\omega_n)}, \quad (87)$$

and in DMFT, the self-energy has no momentum dependence.

We start by deriving the equation of motion for the Green function in Eq. (85) and extracting the expression for the local four-operator correlation function by evaluating the Green function at $\tau = 0$ and removing the single-particle terms,

$$\langle f_i^\dagger f_i c_i^\dagger c_i \rangle = \frac{T}{U} \sum_{n,\mathbf{k}} \Sigma_{\mathbf{k}}(i\omega_n) G_{\mathbf{k}}(i\omega_n). \quad (88)$$

The correlation functions for operators on different sites, such as $\langle f_i^\dagger f_i c_i^\dagger c_j \rangle$, can be found by introducing an extra term $-\Sigma_i h_i f_i^\dagger f_i$ with a local field h_i into the equilibrium Hamiltonian and then evaluating derivatives with respect to h_i and taking the limit $h_i \to 0$. For example, straightforward algebra shows that

$$\langle f_i^\dagger f_i c_i^\dagger c_j \rangle = \left[T \frac{\partial}{\partial h_i} + \langle w_i \rangle \right] G_{ij}(\tau = 0^-), \quad (89)$$

where $\langle w_i \rangle = \langle f_i^\dagger f_i \rangle = n_{fi}$ (see Refs. 17, 41, and 42 and the Appendix for details). Using these identities allows us to find explicit expressions for all of the relevant correlation functions using Green functions and self-energies determined at the Matsubara frequencies. We present the final results for the case of the Falicov–Kimball model in infinite dimensions, where the self-energy is momentum independent,

$$n_c = T \sum_{n,\mathbf{k}} G_{\mathbf{k}}(i\omega_n), \quad (90)$$

$$\sum_{i,j} t_{ij} \langle c_i^\dagger c_j \rangle = -T \sum_{n,\mathbf{k}} \varepsilon(\mathbf{k}) G_{\mathbf{k}}(i\omega_n), \quad (91)$$

$$\sum_{i,l,j} t_{il} t_{lj} \langle c_i^\dagger c_j \rangle = T \sum_{n,\mathbf{k}} \varepsilon^2(\mathbf{k}) G_{\mathbf{k}}(i\omega_n), \quad (92)$$

$$\sum_{i,l,m,j} t_{il} t_{lm} t_{mj} \langle c_i^\dagger c_j \rangle = -T \sum_{n,\mathbf{k}} \varepsilon^3(\mathbf{k}) G_{\mathbf{k}}(i\omega_n), \quad (93)$$

$$\sum_i \langle f_i^\dagger f_i c_i^\dagger c_i \rangle = \frac{T}{U} \sum_{n,\mathbf{k}} \Sigma(i\omega_n) G_{\mathbf{k}}(i\omega_n), \quad (94)$$

$$\sum_{i,j} t_{ij} \langle f_i^\dagger f_i c_i^\dagger c_j \rangle = \left[\sum_{i,j} t_{ji} \langle f_i^\dagger f_i c_j^\dagger c_i \rangle \right]^*$$
$$= -\frac{T}{U} \sum_{n,\mathbf{k}} \Sigma(i\omega_n) \varepsilon(\mathbf{k}) G_{\mathbf{k}}(i\omega_n), \quad (95)$$

$$\sum_{i,l,j} t_{il} t_{lj} \langle c_i^\dagger c_j f_i^\dagger f_i \rangle = \sum_{i,l,j} t_{il} t_{lj} \langle c_i^\dagger c_j f_j^\dagger f_j \rangle = \left[\sum_{i,l,j} t_{ij} t_{jl} \langle c_i^\dagger c_l f_j^\dagger f_j \rangle \right]^*$$
$$= \frac{T}{U} \sum_{n,\mathbf{k}} \Sigma(i\omega_n) \varepsilon^2(\mathbf{k}) G_{\mathbf{k}}(i\omega_n), \quad (96)$$

TABLE I. Retarded moments for $U=3$ (a Mott insulator) and $1/\beta=0.1$ in equilibrium. We used 200 000 positive Matsubara frequencies and 60 000 positive real frequencies with a step size of 0.0002.

U	μ_0^R	μ_1^R	μ_2^R	μ_3^R	C_0^R	C_1^R
3 (Calc.)	1.0000000005	3.1×10^{-17}	2.7500000007	-4.2×10^{-16}	2.2500009	2.9×10^{-17}
3 (Exact)	1.0000000000	0	2.7500000	0	2.2500000	0

$$\sum_{i,j} t_{ij}\langle f_j^\dagger f_j f_i^\dagger f_i c_i^\dagger c_j\rangle = -\frac{T}{U^2}\sum_{n,\mathbf{k}}\Sigma^2(i\omega_n)\varepsilon(\mathbf{k})G_{\mathbf{k}}(i\omega_n). \quad (97)$$

We next perform the momentum summation in Eqs. (90)–(97) to express the results in terms of local quantities,

$$n_c = T\sum_n G_n, \quad (98)$$

$$\sum_{i,j} t_{ij}\langle c_i^\dagger c_j\rangle = T\sum_n \left[1-(i\omega_n+\mu-\Sigma_n)G_n\right], \quad (99)$$

$$\sum_{i,l,j} t_{il}t_{lj}\langle c_i^\dagger c_j\rangle = -T\sum_n (i\omega_n+\mu-\Sigma_n)[1-(i\omega_n+\mu-\Sigma_n)G_n], \quad (100)$$

$$\sum_{i,l,m,j} t_{il}t_{lm}t_{mj}\langle c_i^\dagger c_j\rangle$$
$$= T\sum_n\left[\frac{1}{2}+(i\omega_n+\mu-\Sigma_n)^2(1-(i\omega_n+\mu-\Sigma_n)G_n)\right], \quad (101)$$

$$\sum_i \langle f_i^\dagger f_i c_i^\dagger c_i\rangle = \frac{T}{U}\sum_n \Sigma_n G_n, \quad (102)$$

$$\sum_{i,j} t_{ij}\langle f_i^\dagger f_i c_i^\dagger c_j\rangle = \left[\sum_{i,j} t_{ji}\langle f_i^\dagger f_i c_j^\dagger c_i\rangle\right]^*$$
$$= \frac{T}{U}\sum_n \Sigma_n[1-(i\omega_n+\mu-\Sigma_n)G_n], \quad (103)$$

$$\sum_{i,l,j} t_{il}t_{lj}\langle c_i^\dagger c_j f_j^\dagger f_j\rangle = \left[\sum_{i,l,j} t_{il}t_{lj}\langle c_i^\dagger c_j f_i^\dagger f_i\rangle\right]^* = \sum_{i,l,j} t_{ij}t_{jl}\langle c_i^\dagger c_l f_j^\dagger f_j\rangle$$
$$= -\frac{T}{U}\sum_n \Sigma_n(i\omega_n+\mu-\Sigma_n)$$
$$\times[1-(i\omega_n+\mu-\Sigma_n)G_n], \quad (104)$$

$$\sum_{i,j} t_{ij}\langle f_j^\dagger f_j f_i^\dagger f_i c_i^\dagger c_j\rangle = \frac{T}{U^2}\sum_n \Sigma^2(i\omega_n)[1-(i\omega_n+\mu-\Sigma_n)G_n], \quad (105)$$

where $G_n \equiv \Sigma_{\mathbf{k}}G_{\mathbf{k}}(i\omega_n)$ and $\Sigma_n \equiv \Sigma(i\omega_n)$. These expressions can then be employed to efficiently determine the lesser moments from an independent Matsubara frequency calculation.

We find, for all cases that we consider, all of the different Green function and self-energy moment sum rules are satisfied to essentially as high an accuracy as we want (the delta-function contributions to the self-energy moments must be included to get the correct answer; this becomes complicated for particle-hole asymmetric cases when U is large enough for the self-energy to have developed a pole because one needs to accurately determine the location and weight of the pole to obtain the correct sum rules). In some cases, we need to use many Matsubara frequencies in the summations to achieve sufficient accuracy or we need to have a small frequency grid spacing for the real-frequency Green functions. The sum rules hold in the case of half-filling and away from particle-hole symmetry and they hold equally well for metallic and insulating cases. As an example, we tabulate the sum rules for a Mott insulating phase at half-filling in Table I (retarded) and Table II (lesser). Results for metallic cases are similar.

B. Nonequilibrium case

In this section, we compare the numerical results for the moments (at half-filling) with exact analytical results obtained in the case when a constant electric field is turned on at time $T=0$. Since we calculate the contour-ordered self-energy, we need to extract the correct retarded quantities to compare with the moments that do not depend on correlation functions (which we have no independent way to evaluate). This is simple to do for the Green functions. For the self-energies, care is needed. The constant term in the self-energy in the frequency representation becomes an equal-time delta function in the time formalism. The zeroth moment corresponds to the equal-time retarded self-energy (most easily found by taking the difference of the greater and lesser self-energies) and the first moment is found from the first derivative. We need to carefully evaluate the derivative because we need to remove the delta-function piece first. We handle this instead by using linear extrapolation from finite relative times to the vanishing relative-time limit, so we do not need

TABLE II. Lesser moments for $U=3$ (a Mott insulator) and $1/\beta=0.1$ in equilibrium. We used 200 000 positive Matsubara frequencies and 60 000 positive real frequencies with a step size of 0.0002. Note how it is more difficult to get high accuracy for the odd moments.

U	$\mu_0^<$	$\mu_1^<$	$\mu_2^<$	$\mu_3^<$
3 (Calc.)	1.0000000005	-1.5821717	2.7500000007	-5.1601698
3 (Exact)	1.0000000000	-1.5821578	2.7500000000	-5.1578586
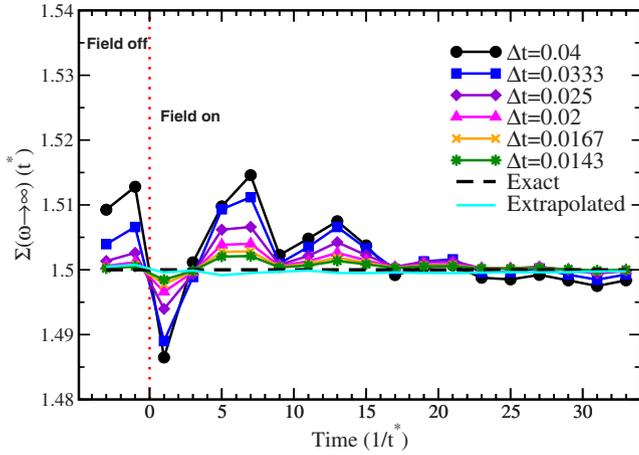
FIG. 2. (Color online) Constant piece of the retarded self-energy $\Sigma^R(\omega \rightarrow \infty)$ as a function of average time. The curves with symbols correspond to nonequilibrium calculations with different discretization sizes Δt on the real part of the Kadanoff–Baym–Keldysh contour. The dashed line is the exact result (equal to 1.5 here) and the solid line with no symbols is the extrapolated result using a quadratic extrapolation with the three smallest discretization sizes. The parameters are $E=1$, $U=3$, and $1/\beta=0.1$; the calculation is done at half-filling for both the delocalized and the localized particles. Note how the extrapolated result is accurate to better than 0.1%.

the data at equal times to find the derivative. More sophisticated techniques would be needed to find the higher moments, but we do not need those here.

In general, the self-energy moments are satisfied to very high accuracy even if the step size is large. Errors are often less than 0.1%, which is much lower than what one finds for the Green function moments (where we often need to work hard to get errors below the 1% level[18,19,21]). We can extrapolate the results to the limit $\Delta t \rightarrow 0$, which produces even higher accuracy. The results are most accurate for the constant piece to the self-energy, then the zeroth moment and, finally, the first moment. However, the results of our investigations indicate that the Green function moments are a much more accurate test of the accuracy of the solutions than the self-energy moments. To illustrate this, we show similar scaling plots to those already published[18] for the Green function moments with $E=1$ and $U=3$ in Figs. 2–4. One can see that the accuracy for the self-energy is very high even though this case is a strong Mott insulator, where the numerics require results at many different step sizes to be able to extrapolate to the continuous $\Delta t \rightarrow 0$ limit. Indeed, the accuracy for the self-energy appears to be at least an order of magnitude better than for the Green function in most cases. Also, we find, once again, that the accuracy is worse in the equilibrium region before the field is turned on (negative times).

VI. CONCLUSIONS

In this work, we have shown how to extend the Green function moment sum rules to third order for both the Hubbard and the Falicov–Kimball models and used these moments to examine the retarded self-energy moments through first order. Our analysis holds both for equilibrium and non-
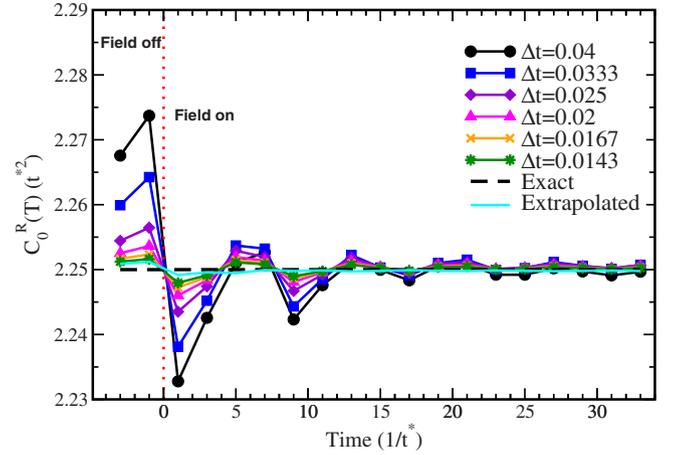
FIG. 3. (Color online) Zeroth moment of the retarded self-energy $C_0^R(T)$ as a function of average time. The curves with symbols correspond to nonequilibrium calculations with different discretization sizes Δt on the real part of the Kadanoff–Baym–Keldysh contour. The dashed line is the exact result (equal to 2.25 here) and the solid line with no symbols is the extrapolated result using a quadratic extrapolation with the three smallest discretization sizes. The parameters are $E=1$, $U=3$, and $1/\beta=0.1$; the calculation is done at half-filling for both the delocalized and the localized particles. Note how the extrapolated result is accurate to better than 0.1%.

equilibrium situations. We find for the Falicov–Kimball model that the moment sum rules remain time independent in nonequilibrium, which is a surprising result. In the case of the Hubbard model, it appears that the third order moments will be time dependent, but we cannot explicitly confirm this. When we compare the sum rules to numerical calculations
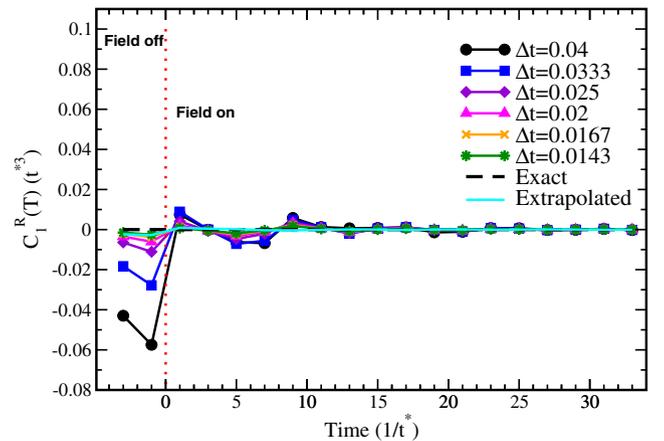
FIG. 4. (Color online) First moment of the retarded self-energy $C_1^R(T)$ as a function of average time. The curves with symbols correspond to nonequilibrium calculations with different discretization sizes Δt on the real part of the Kadanoff–Baym–Keldysh contour. The dashed line is the exact result (equal to 0 here) and the solid line with no symbols is the extrapolated result using a quadratic extrapolation with the three smallest discretization sizes. The parameters are $E=1$, $U=3$, and $1/\beta=0.1$; the calculation is done at half-filling for both the delocalized and the localized particles. Note how the extrapolated result has high accuracy.

for the Falicov–Kimball model with DMFT, we find excellent agreement both in equilibrium and in nonequilibrium. In fact, the Green function sum rules are a much better indicator of overall accuracy than the self-energy sum rules.

The sum rules are only relevant for quantitative comparisons of retarded functions. In the case of lesser functions, we are able to make comparisons of the Green function sum rules to the relevant correlation functions evaluated with a Matsubara frequency formalism when the system is in equilibrium, but we cannot extend that approach to the nonequilibrium case. We are unable, even in equilibrium, to find any useful sum rules for the lesser self-energy. Instead, we find just trivial relationships that arise from the definitions of these quantities (which are well known in equilibrium and unknown in nonequilibrium).

In the future, we will examine how these sum rules can be extended to inhomogeneous situations, with relevance to inhomogeneous DMFT (and other techniques) as applied to mutlilayered nanostructures or ultracold atomic systems in a harmonic trap. In addition, utilizing these sum rules can allow one to obtain more accurate results for the high-frequency limit of the Green functions, self-energies, and dynamical mean fields. We will illustrate this use in another publication, which allows one to employ a minimal number of Matsubara frequencies yet maintain high accuracy of solutions.

APPENDIX: CALCULATION OF EQUILIBRIUM CORRELATION FUNCTIONS USING THE MATSUBARA FREQUENCY FORMALISM

In this appendix, we present details of the derivation of the correlation functions in Eqs. (94)–(97). The expression in Eq. (88) for the first correlation function in Eq. (94) can also be determined by introducing a fictitious field $-\Sigma_i h_i f_i^\dagger f_i$ into the Hamiltonian and taking derivatives with respect to h_i and then setting all $h_i=0$. Each derivative with respect to an h_i brings down an operator $f_i^\dagger f_i$ into the operator average (plus a correction term when the derivative acts on the partition function in the denominator of the thermal average). This approach is more general than the equation of motion approach used to derive Eq. (88) and will allow us to derive expressions for the other correlation functions in Eqs. (95)–(97). As shown in Ref. 42, a correlation function that contains a product of two c-electron operators and one f-electron number operator can be expressed in terms of a derivative of the c-electron Green function with respect to the fictitious field [see, for example, Eq. (89)].

In order to explicitly calculate the fictitious field derivative of the Green function, one uses the standard trick of writing $G=GG^{-1}G$ so that derivatives of G are replaced by derivatives of G^{-1}, which involve a derivative of the self-energy (see Ref. 42). Because we have added the fictitious fields to the Hamiltonian, and they are not translationally invariant, we lose translational invariance in the system prior to taking the derivatives (it is restored once we set $h_i=0$). Hence, we need to work in real space rather than momentum space, and we need to allow the dynamical mean fields and the self-energies to have a site dependence. This implies that we can write the local Green function at site i via

$$G_{ii}(i\omega_n) = \frac{1}{i\omega_n + \mu - \lambda_i(i\omega_n) - \Sigma_i(i\omega_n)}, \qquad \text{(A1)}$$

in the Matsubara frequency representation.

Now, consider the case where we add an h field only at site i. Since the h field will modify n_{fi}, the Green function and self-energy at site i are changed by h_i. What about the Green function and self-energy on neighboring sites? By using the Dyson equation, one can show that the change in the Green function at site j, $\delta G_{jj}(i\omega_n)$, is equal to

$$\delta G_{jj}(i\omega_n) = G_{ji}(i\omega_n)|_{h_i=0} \delta\Sigma_i(i\omega_n) G_{ij}(i\omega_n)|_{h_i=0}. \quad \text{(A2)}$$

However, G_{ij} is proportional to the hopping t raised to the power equal to the smallest number of hops between site i and site j. So, for example, if j is a nearest neighbor of site i, the right hand side of Eq. (A2) is proportional to $t^2 = t^{*2}/4d \to 0$ as $d \to \infty$. Hence, we learn that $\delta G_{jj}(i\omega_n)=0$ for $j \neq i$ and large dimensions. If G_{jj} is unchanged, then Σ_j is also unchanged. This means that

$$\frac{\partial \Sigma_j(i\omega_n)}{\partial h_i} \propto \delta_{ij}. \qquad \text{(A3)}$$

We now show how to derive one of the off-diagonal c-f correlation functions. We want to calculate

$$\sum_{ij} t_{ij} \langle f_i^\dagger f_i c_i^\dagger c_j \rangle = \frac{1}{\beta} \sum_n \sum_{ij} \left[\frac{\partial}{\beta \partial h_i} + n_{fi} \right] G_{ji}(i\omega_n), \quad \text{(A4)}$$

which directly follows from the definition of the operator average and an explicit computation of the derivative (the term multiplied by n_{fi} arises from the derivative of the partition function). Now, we focus on the derivative term and use the $GG^{-1}G$ trick,

$$\frac{\partial}{\beta \partial h_i} G_{ji}(i\omega_n) = \frac{\partial}{\beta \partial h_i} \sum_{kl} G_{jk}(i\omega_n) G_{kl}^{-1}(i\omega_n) G_{li}(i\omega_n),$$
$$\text{(A5)}$$

$$= G_{ji}(i\omega_n) \left[\frac{\partial}{\beta \partial h_i} \Sigma_i(i\omega_n) \right] G_{ii}(i\omega_n), \qquad \text{(A6)}$$

where we used the fact that the derivative of the self-energy was nonzero only for $k=l=i$. Since the self-energy is an implicit function of G_{ii} and n_{fi}, one can compute the derivative of the self-energy with respect to the field by using the chain rule and re-expressing in terms of derivatives of the self-

energy with respect to the Green function and the f-electron filling. The algebra is quite long and is contained in Ref. 42. The end result is that

$$G_{ii}(i\omega_n)\left[\frac{\partial}{\beta\partial h_i}\Sigma_i(i\omega_n)\right] + n_{fi} = \frac{\Sigma_i(i\omega_n)}{U}. \quad (A7)$$

Plugging this result into Eq. (A6) and then converting the summation over i and j to a summation over momentum produces Eq. (95).

The only equation that requires some more formal development is Eq. (97) because it involves two f-electron density operators and, hence, derivatives with respect to two h fields. By using the fictitious fields, one can immediately show that

$$\sum_{ij} t_{ij}\langle f_j^\dagger f_j f_i^\dagger f_i c_i^\dagger c_j\rangle = \sum_{ij} t_{ij}\left[\frac{\partial}{\beta\partial h_j} + n_{fj}\right]$$

$$\times \left[\frac{\partial}{\beta\partial h_i} + n_{fi}\right]G_{ji}(\tau = 0^-). \quad (A8)$$

All the terms in this expression, except the term proportional $\partial^2 G_{ji}/\partial h_j\partial h_i$, can be expressed in terms of the Green function and self-energies by using the results above. In order to find the second derivative of the Green function, one can show

(similar to the case of the first derivative) that in the limit of infinite dimensions,

$$\frac{\partial^2 G_{ji}(i\omega_n)}{\partial h_j\partial h_i}\bigg|_{h=0} = \frac{\partial}{\partial h_j}\left[G_{ii}(i\omega_n)G_{ji}(i\omega_n)\frac{\partial\Sigma_i}{\partial h_i}\right]\bigg|_{h=0}$$

$$= G_{ii}(i\omega_n)G_{jj}(i\omega_n)G_{ji}(i\omega_n)\ \frac{\partial\Sigma_j}{\partial h_j}\frac{\partial\Sigma_i}{\partial h_i}\bigg|_{h=0}$$

$$+ G_{jj}(i\omega_n)G_{ji}(i\omega_n)\ \frac{\partial^2\Sigma_i}{\partial h_j\partial h_i}\bigg|_{h=0}. \quad (A9)$$

The last term in this equation is equal to zero since the second derivative of the self-energy $\partial^2\Sigma_i(i\omega_n)/\partial h_j\partial h_i$ vanishes. The argument is elementary. Note that $\partial\Sigma_j/\partial h_j$ is a function of G_{jj} and Σ_j. If we now take a derivative with respect to h_i when $i \neq j$, the derivative must vanish because the derivative of G_{jj} and Σ_j with respect to h_i is zero. Therefore,

$$\frac{\partial^2 G_{ji}(i\omega_n)}{\partial h_j\partial h_i}\bigg|_{h=0} = G_{ii}(i\omega_n)G_{jj}(i\omega_n)G_{ji}(i\omega_n)\ \frac{\partial\Sigma_j}{\partial h_j}\frac{\partial\Sigma_i}{\partial h_i}\bigg|_{h=0}.$$

$$(A10)$$

Evaluating the derivatives explicitly and simplifying the final result then yields Eq. (97).

---

*turkowskiv@missouri.edu

†URL: http://www.physics.georgetown.edu/~jkf

[1] Y. Tokura, Phys. Today **56**(7), 50 (2003).

[2] J. Hubbard, Proc. R. Soc. London, Ser. A **276**, 238 (1963).

[3] L. M. Falicov and J. C. Kimball, Phys. Rev. Lett. **22**, 997 (1969).

[4] E. H. Lieb and F. Y. Wu, Phys. Rev. Lett. **20**, 1445 (1968).

[5] A. Georges, G. Kotliar, W. Krauth, and M. J. Rozenberg, Rev. Mod. Phys. **68**, 13 (1996).

[6] J. K. Freericks and V. Zlatić, Rev. Mod. Phys. **75**, 1333 (2003).

[7] Y. Meir, N. S. Wingreen, and P. A. Lee, Phys. Rev. Lett. **70**, 2601 (1993).

[8] Y. Taguchi, T. Matsumoto, and Y. Tokura, Phys. Rev. B **62**, 7015 (2000).

[9] T. Oka, R. Arita, and H. Aoki, Phys. Rev. Lett. **91**, 066406 (2003).

[10] T. Oka and H. Aoki, Phys. Rev. Lett. **95**, 137601 (2005).

[11] P. Mehta and N. Andrei, Phys. Rev. Lett. **96**, 216802 (2006).

[12] U. Schollwöck, Rev. Mod. Phys. **77**, 259 (2005).

[13] P. Schmidt and H. Monien, arXiv:cond-mat/0202046 (unpublished).

[14] P. Schmidt, Diplome thesis, University of Bonn, 2002.

[15] V. Turkowski and J. K. Freericks, Phys. Rev. B **75**, 125110 (2007).

[16] J. K. Freericks, V. M. Turkowski, and V. Zlatić, in *Proceedings of the HPCMP Users Group Conference 2005, Nashville, TN, 28–30 June 2005*, edited by D. E. Post (IEEE Computer Society, Los Alamitos, CA, 2005), pp. 25–34.

[17] V. M. Turkowski and J. K. Freericks, Phys. Rev. B **73**, 075108 (2006); **73**, 209902(E) (2006).

[18] J. K. Freericks, V. M. Turkowski, and V. Zlatić, in *Proceedings of the HPCMP Users Group Conference 2006, Denver, CO,*

26–29 June 2006, edited by D. E. Post (IEEE Computer Society, Los Alamitos, CA, 2006), pp. 218–226.

[19] J. K. Freericks, V. M. Turkowski, and V. Zlatić, Phys. Rev. Lett. **97**, 266408 (2006).

[20] V. M. Turkowski and J. K. Freericks, in *Strongly Correlated Systems, Coherence and Entanglement*, edited by J. M. P Carmelo, J. M. B. Lopes dos Santos, V. Rocha Vieira, and P. D. Sacramento (World Scientific, Singapore, 2007), pp. 187–210.

[21] J. K. Freericks, Phys. Rev. B **77**, 075109 (2008).

[22] M. Eckstein and M. Kollar, Phys. Rev. Lett. **100**, 120404 (2008).

[23] S. R. White, Phys. Rev. B **44**, 4670 (1991).

[24] A. B. Harris and R. V. Lange, Phys. Rev. **157**, 295 (1967).

[25] W. Nolting, Z. Phys. **255**, 25 (1972).

[26] G. Geipel and W. Nolting, Phys. Rev. B **38**, 2608 (1988).

[27] W. Nolting and W. Borgiel, Phys. Rev. B **39**, 6962 (1989).

[28] M. Potthoff, T. Wegner, and W. Nolting, Phys. Rev. B **55**, 16132 (1997).

[29] M. Potthoff, T. Herrmann, T. Wegner, and W. Nolting, Phys. Status Solidi B **210**, 199 (1999).

[30] H. Eskes, A. M. Oles, M. B. J. Meinders, and W. Stephan, Phys. Rev. B **50**, 17980 (1994).

[31] O. Rosch, G. Sangiovanni, and O. Gunnarson, Phys. Rev. B **75**, 035119 (2007).

[32] M. Randeria, R. Sensarma, N. Trivedi, and F.-Ch. Zhang, Phys. Rev. Lett. **95**, 137001 (2005).

[33] P. E. Kornilovitch, Europhys. Lett. **59**, 735 (2002).

[34] R. E. Peierls, Z. Phys. **80**, 763 (1933); A. P. Jauho and J. W. Wilkins, Phys. Rev. B **29**, 1919 (1984).

[35] V. M. Turkowski and J. K. Freericks, Phys. Rev. B **71**, 085104 (2005).

[36] J. J. Deisz, D. W. Hess, and J. W. Serene, Phys. Rev. B **55**, 2089

(1997).

[37] J. K. Freericks, D. O. Demchenko, A. V. Joura, and V. Zlatić, Phys. Rev. B **68**, 195120 (2003).

[38] P. Lipavský, V. Spicka, and B. Velický, Phys. Rev. B **34**, 6933 (1986).

[39] W. Metzner, Phys. Rev. B **43**, 8549 (1991).

[40] M. Jarrell, Phys. Rev. Lett. **69**, 168 (1992).

[41] J. K. Freericks and V. Zlatić, Phys. Rev. B **58**, 322 (1998).

[42] J. K. Freericks and V. Zaltić, Phys. Rev. B **64**, 245118 (2001).